

Supplementary Information

Photodynamic therapy photosensitizers and photoactivated chemotherapeutics exhibit distinct bioenergetic profiles to impact ATP metabolism

Richard J. Mitchell, Dmytro Havrylyuk, Austin C. Hachey, David K. Heidary*, and Edith C. Glazer*

Experimental Methods

Figures:

Figure S1. Cytotoxicity curves of the Ru(II) compounds investigated in this study.

Figure S2. Chromatograms of **1** – **13** for log P determination.

Figure S3. Standard curve used to determine relative log P for each compound in this study.

Figure S4. The correlation between log P and cytotoxicity.

Figure S5. Extracellular flux analysis of compounds **1** – **12** in the absence of indigo light.

Figure S6. Extracellular flux analysis of compounds **1** – **12** following exposure to indigo light.

Figure S7. Extracellular flux analysis of compounds **13** – **15**.

Figure S8. Glycolytic Rate Test following a 1 h incubation with **2** and **6** in the dark and with indigo light.

Figure S9. Glycolytic Rate Test in the dark and with red light with HPPH.

Figure S10. Concentration dependent bioenergetic impacts of phototherapeutics in A549 cells.

Figure S11. Concentration dependent bioenergetic impacts of compounds that can generate $^1\text{O}_2$ in A549 cells.

Figure S12. Concentration dependent bioenergetic impacts of compounds that photoeject in A549 cells.

Figure S13. Photoejection UV/Vis of compounds **2**, **4**, **5**, **7**, **11**, and **12** over 60 seconds with indigo light.

Figure S14. Photoejection of compounds **2**, **4**, **5**, **7**, **11**, and **12** monitored by HPLC.

Figure S15. Mass spectra of the parent complex **2** and its photoejection products.

Figure S16. Mass spectra of the parent complex **4** and its photoejection products.

Figure S17. Mass spectra of the parent complex **5** and its photoejection products.

Figure S18. Mass spectra of the parent complex **11** and its photoejection products.

Figure S19. Mass spectra of the parent complex **12** and photoejection products.

Figure S20. Production of $^1\text{O}_2$ as detected by SOSG for **1**, **7**, and **12**.

Figure S21. Key parameters of the MitoStress Test after a 1 h incubation with dark active compounds.

Table S1. Relative lipophilicity of the compounds in this study.

Table S2. Photoconversion efficiency of the PACTs in this study.

Experimental Methods

General

All compounds except phenanthriplatin and the Ru(II) complexes were purchased from commercial sources. The sources are as follows: Gleevec (Enzo Life sciences); bleomycin, cycloheximide (CHX), and actinomycin D, Cayman Chemical; doxorubicin, Fisher; cisplatin and CX-5461 (Sigma-Aldrich). Phenanthriplatin was synthesized as previously reported.¹ All ruthenium-based agents were synthesized as previously reported.²⁻⁶ Most agents were prepared as either 10 or 20 mM solutions in dimethyl sulfoxide (DMSO) and stored at -20 °C. Cisplatin and phenanthriplatin were prepared as 3 mM and 10 mM stocks in phosphate-buffered saline (pH = 7.4) and stored at -20 °C. Fetal bovine serum (FBS) was purchased from Corning. Streptomycin and penicillin were purchased from Cytiva. Dulbecco's modified eagle medium (DMEM) was purchased from Cytiva. Light activation experiments were performed using a 450 nm flood array from Loctite or a 660 nm LED array from Elixia. For the 660 nm LED, peak emission $\lambda_P = 660$ nm, spectral line full width at half-maximum $\Delta\lambda = 20$ nm. Cytotoxicity measurements were collected on a Tecan Spectrafluor and Magellan Pro (version 3.1). A Seahorse Extracellular Flux Analyzer Fe96 was used for all cellular respiration measurements. The Seahorse data was processed on Wave (version 2.6.3), Microsoft Excel (2016 version), and GraphPad Prism (version 9.3.1).

HPLC analysis for purity, lipophilicity, and photoejection products

The purity of each compound was analyzed using an Agilent 1100 Series HPLC equipped with a model G1311A quaternary pump, G1315B UV diode array detector, and Chemstation software version B.01.03. Chromatographic conditions were optimized on a Phenomenex Luna C18(2), 100 Å (250 × 4.6 mm inner diameter, 5 μM) fitted with a Phenomenex C18 (4 × 3 mm) guard column. An injection volume of 20 μL of 100 μM solution of each compound was used. The detection wavelength was 280 nm. Mobile phases were: mobile phase A, 0.1% formic acid in diH₂O; mobile phase B, 0.1% formic acid in HPLC grade acetonitrile. The mobile phase flow rate was 1.0 mL/min. The following mobile phase gradient was used: 98–95% A (containing 2–5% B) from 0 to 5 min; 95–70% A (5–30% B) from 5 to 15 min; 70–40% A (30–60% B) from 15 to 20 min; 40–5% A (60–95% B) from 20 to 30 min; 5–98% A (95–2% B) from 30 to 35 min; re-equilibration at 98% A (2% B) from 35 to 40 min.

The photoejection products were determined via an Agilent LC-MS (G6125BA). The photoejection products were resolved using the following gradient: 98–95% A (2–5% B) from 0 to 3 min; 95–70% A (5–30% B) from 3 to 9 min; 70–40% A (30–60% B) from 9 to 12 min; 40–5% A (60–95% B) from 12 to 18 min; 5–98% A (95–2% B) from 18 to 21 min; re-equilibration at 98% A (2% B) from 21 to 25 min. The mass spectrometer collected spectra in dual polarity mode, scanning 100–1,500 m/z with a cycle time of 1.1 seconds per cycle.

Counter-ion exchange

Before photoejection studies and biological testing, counterion exchange was performed on each Ru(II) complex. The PF₆⁻ counterion was converted to the Cl⁻ salt by dissolving 10 mg of product in 2 mL methanol. The dissolved product was loaded onto an Amberlite IRA-410 chloride ion exchange column, eluted with methanol, and the solvent was removed *in vacuo*.

Lipophilicity measurements

The retention times for each compound were determined by HPLC as described above. The retention time was correlated to a Log P value using the function $x = (y - .2033)/0.108$, where y is retention time and x is log(P).

Cell Line Maintenance

The A549 (lung adenocarcinoma) cancer cell line was obtained from the American Type Culture Collection (ATCC). The A549 cells were maintained in DMEM media supplemented with 10% FBS, penicillin (100 U/mL), and streptomycin (100 µg/mL), and cultured at 37 °C with 5% CO₂. All studies were conducted when cells were between passage numbers 10 and 18.

Cell Cytotoxicity

The A549 cells were seeded into 96-well plates at 2,000 cells/well in DMEM media supplemented with 10% FBS, penicillin (100 U/mL), and streptomycin (100 µg/mL), and allowed to adhere to the well for 16 h. After the cells adhered to the 96-well plate, the DMEM was aspirated and replaced with extracellular solution (10 mM HEPES, 10 mM glucose, 1.2 mM CaCl₂, 1.2 mM MgCl₂, 3.3 mM KH₂PO₄, 0.83 mM K₂HPO₄, and 145 mM NaCl in deionized water). Compounds were serially diluted in extracellular solution and added to the cells. Following compound addition, cells were irradiated with either 29.1 J/cm² of indigo light (450 nm) or 57.8 J/cm² of red light (660 nm), then an equal volume of Opti-MEM™ supplemented with 4% FBS, penicillin (100 U/mL), and streptomycin (100 µg/mL) was added to the cells, and the cells were allowed to incubate for 72 h at 37 °C with 5% CO₂. After the 72-h incubation, resazurin was added to the cells (73 µM final concentration). Cells were further incubated for 3 h at 37 °C with 5% CO₂ to allow for the reduction of resazurin to resorufin by viable cells. Cell viability was then quantified by measuring fluorescence emission at 595 nm (λ_{ex} : 535 nm) on a SpectraFluor Plus plate reader (Tecan). Cytotoxicity was measured in triplicate (n = 3). Reported as the mean +/- standard deviation.

MitoStress Test

All Seahorse XFe96 experiments were performed with A549 cells. The A549 cells were seeded in a Seahorse XFe96-well plate (Agilent) at 2.5x10⁴ cells in 80 µL of DMEM supplemented with 10% FBS, penicillin (100 U/mL), and streptomycin (100 µg/mL) per well. The plates were set at room temperature for 1 hour to allow cells to settle and then placed in a 37 °C incubator with 5% CO₂ overnight. The next day, DMEM was aspirated from the cells and replaced with 100 µL of each compound in extracellular buffer. Each compound was prepared as a 1% DMSO solution. The cells were incubated with compound for one hour. For the red-light active compound, cells were irradiated during the 1h incubation (660 nm, 57.8 J/cm²). For the blue-light active compounds, A549 cells were irradiated following a 1h incubation (450 nm, 29.1 J/cm²). Following irradiation, the extracellular buffer was aspirated and Opti-MEM supplemented with 2% FBS, penicillin (100 U/mL), and streptomycin (100 µg/mL) was added to the cells. After fifteen minutes, the media was aspirated and replaced with Seahorse XF DMEM Medium (pH = 7.4) supplemented with 25 mM XF Glucose, 2 mM XF Glutamine, and 1 mM XF Pyruvate and cells were incubated at 37°C for 1 h in a CO₂-free incubator before running the assay. The assay was performed using a pneumatic injection for oligomycin, carbonyl cyanide-p-trifluoro-methoxy-phenylhydrazone (FCCP), rotenone, and Antimycin A. Recordings were initiated and oligomycin (1.0 µM) was injected at 18 min. This was followed by an injection of FCCP (1.2 µM) at 36 min and a rotenone/antimycin A cocktail (1.0 µM) at 54 min. A minimum of four replicates (n ≥ 4) were collected for all Mitochondrial Stress Tests. Seahorse experiments were done at the University of Kentucky Markey Cancer Center Redox Metabolism Facility.

Key Terms:

ECAR: Extracellular acidification rate of cells

OCR: Oxygen consumption rate of cells

Basal glycolysis: The rate of the process of converting glucose to lactate under standard conditions.

Compensatory glycolysis: The rate of glycolysis in cells following the addition of mitochondrial inhibitors, effectively inhibiting oxidative phosphorylation and driving compensatory changes in the cell to use glycolysis to meet the cells' energy demands.

Proton efflux rate (PER): The number of protons exported by cells into the assay medium over time, expressed as pmol/min.

Glycolytic Rate Test

The A549 seeding and pre-treatment conditions were the same as described in the MitoStress Test section. The assay was performed using pneumatic injections of rotenone, Antimycin A, and 2-deoxyglucose (2-DG). Recordings were initiated and a rotenone/antimycin A cocktail (1.0 μM each) was injected at 18 min. This was followed by an injection of 2-DG (1.0 μM) at 36 min. A minimum of four replicates ($n \geq 4$) were measured for all Glycolytic Rate Tests. Seahorse experiments were done at the University of Kentucky Markey Cancer Center Redox Metabolism Facility.

Statistical Analysis

All results were analyzed using Excel (Microsoft Office, Version 2016) and expressed as average \pm standard deviation. Statistical significance was evaluated in GraphPad Prism (Version 9.3.1) for the MitoStress and Glycolytic Rate analyses by a one-way ANOVA with Dunnett's multiple comparisons test, P-value ($P < 0.05$ (*), $P < 0.01$ (**), $P < 0.001$ (***) or $P < 0.0001$ (****)).

SOSG Assay

The Singlet Oxygen Sensor Green (SOSG) kit was obtained from Molecular Probes. The SOSG dye was diluted in 33 μL of methanol to create a 5 mM stock solution. Compounds were diluted in PBS and added to a 96-well plate, followed by the addition of SOSG. The concentration of 5 μM was used for both the compounds and SOSG dye in the assay. The plate was read in a BMG Labtech FLUOstar Omega microplate reader with an excitation of 485 nm and an emission of 530 nm. First, the background fluorescence was quantified before the samples were subjected to light irradiation; after this, the plate was irradiated under 445 nm light for 2 min (1.8 J/cm^2) and emission read on the plate reader for a second time. The singlet oxygen level was determined by calculating the ratio from the signal observed before and after light irradiation for each sample.

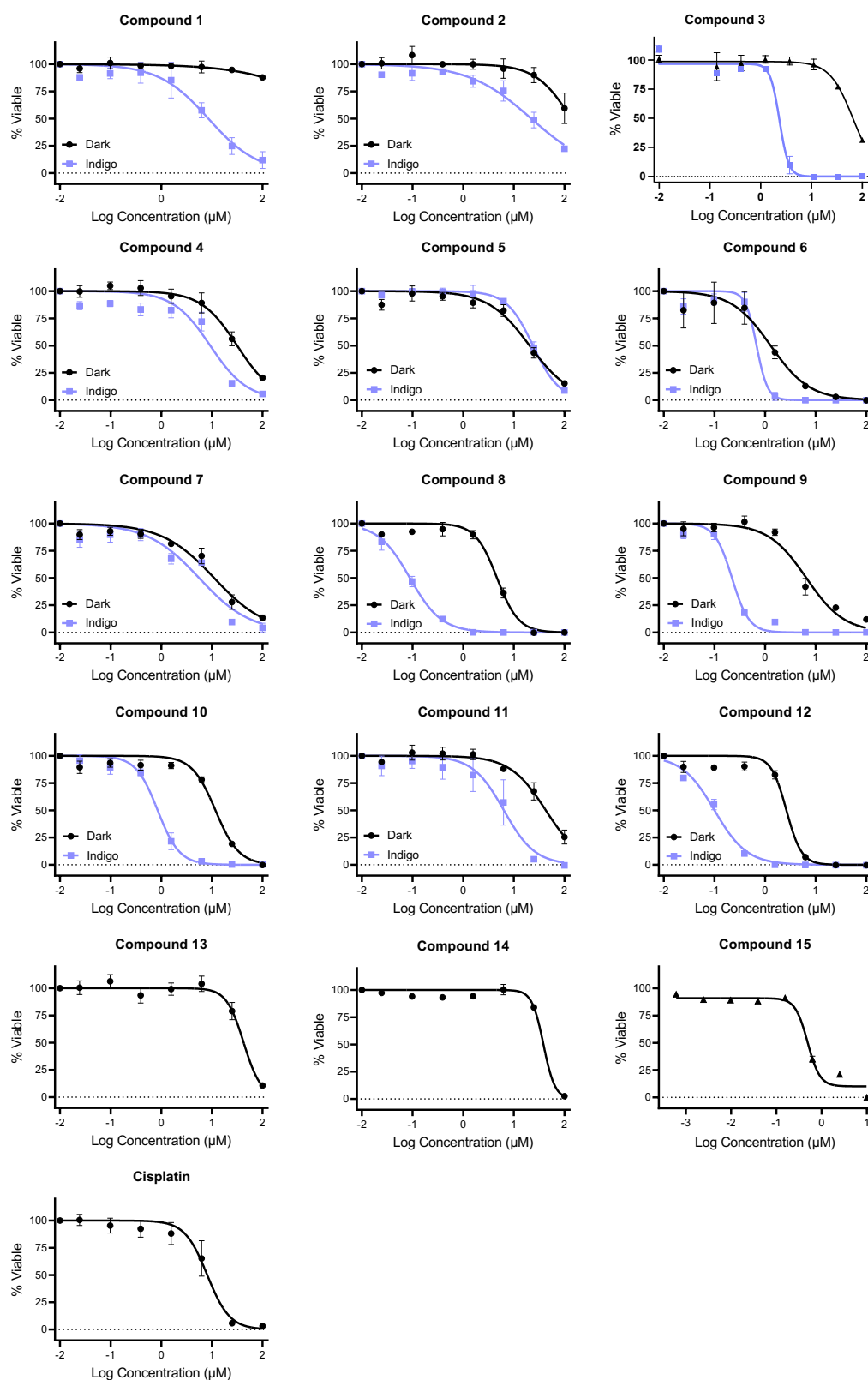


Figure S1. Cytotoxicity curves of the Ru(II) compounds investigated in this study. The A549 cells were treated with 29.1 J/cm² of indigo light. The cytotoxicity of each compound was evaluated after 72 h. Cisplatin was used as a reference (n = 3).

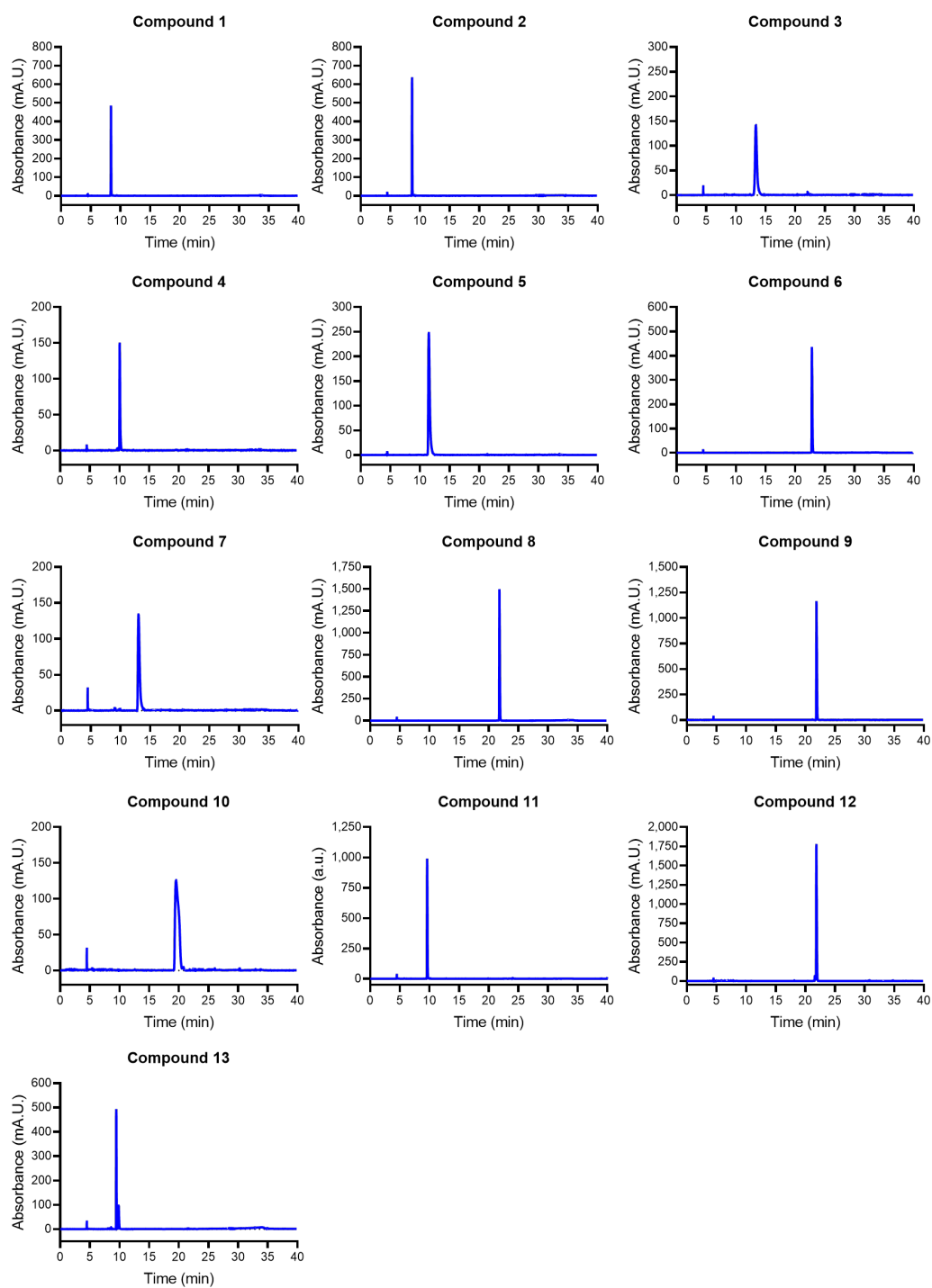


Figure S2. Chromatograms of **1** – **13** for log P determination. The peak at 4.9 minutes is the void volume. Solutions of each compound (100 μ M) were prepared in water prior to injection. Compounds **14** and **15** retention times were obtained from previous reports.⁷

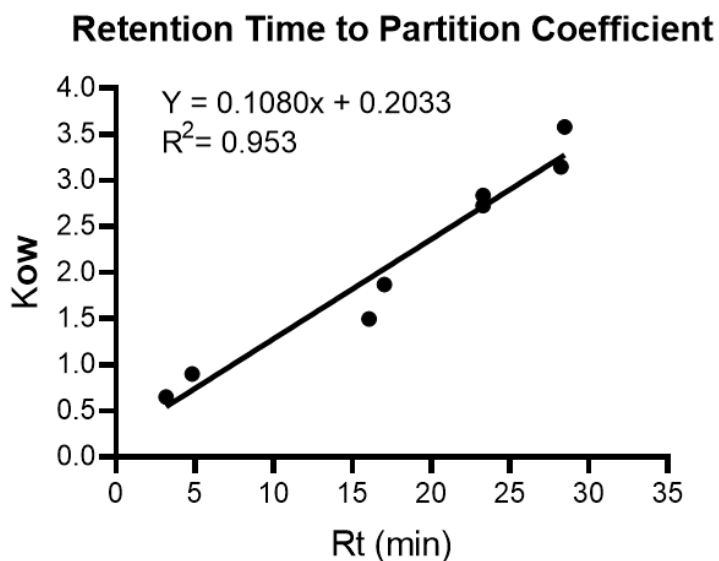


Figure S3. Standard curve used to determine relative log P for each compound in this study.

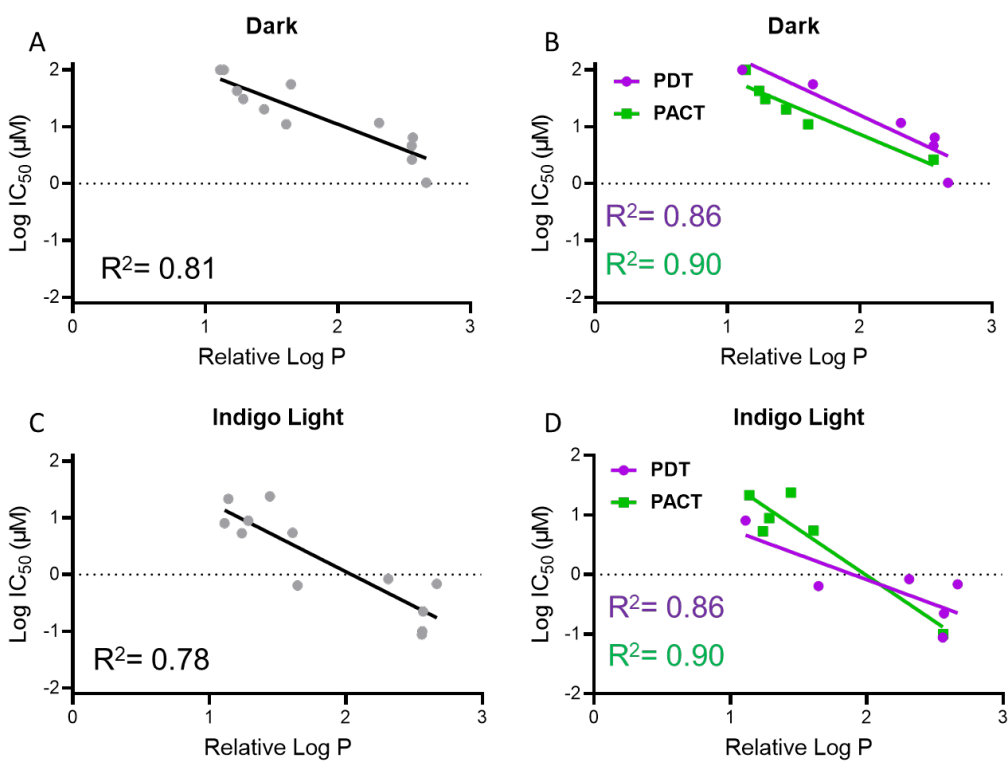


Figure S4. Correlation between relative log P and log IC₅₀ of the Ru(II) investigated. **A)** The log P and cytotoxicity correlation for 1–15 in the dark. **B)** The log P and cytotoxicity correlation coefficient of 1–15 after irradiation (29.1 J/cm²). **C)** The log P and cytotoxicity correlation of the PDT PSs and PACTs as separate categories in the dark. **D)** The log P and cytotoxicity correlation of the PDT PSs and PACTs after irradiation (29.1 J/cm²).

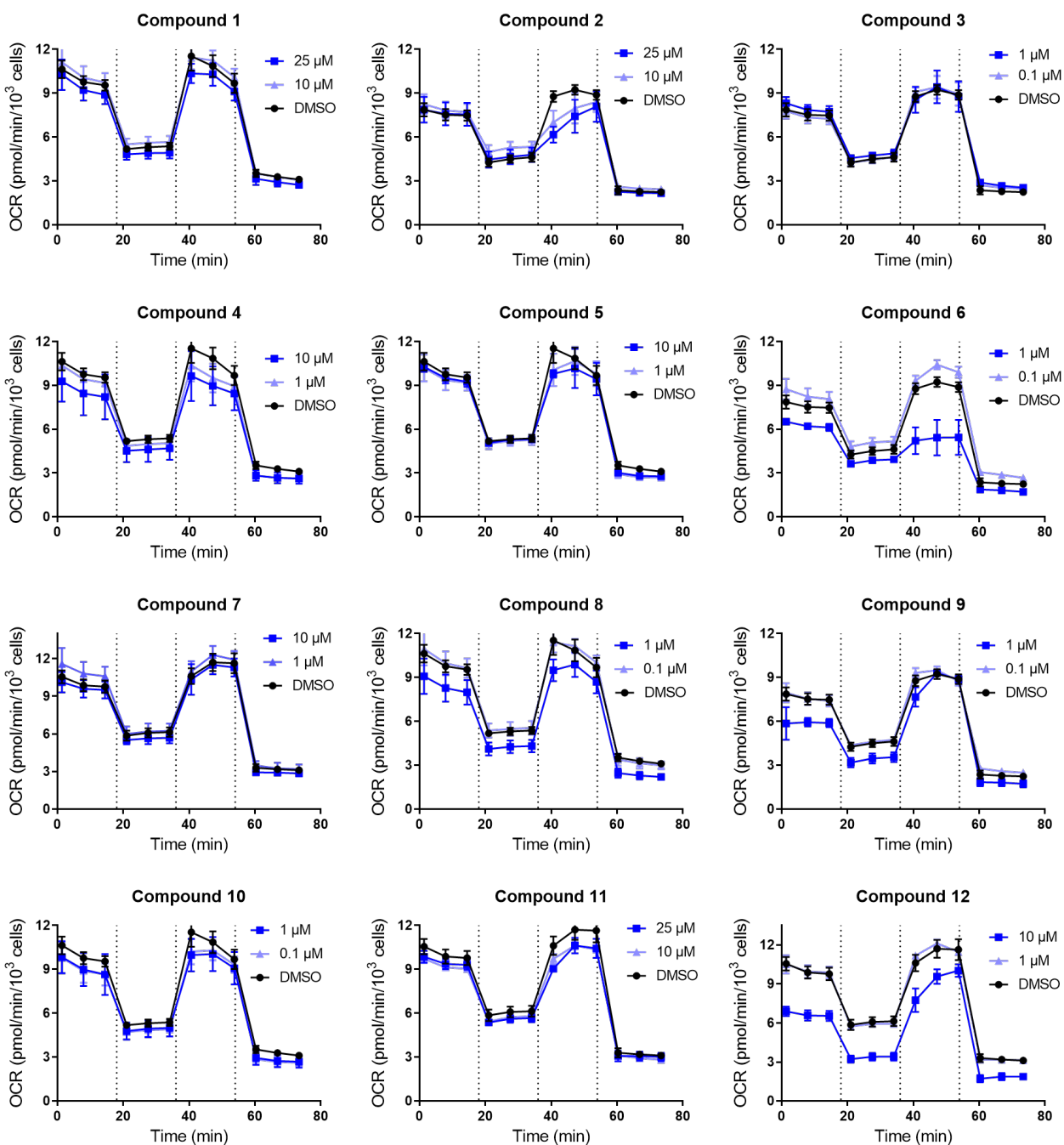


Figure S5. Extracellular flux analysis of compounds 1 – 12 in the absence of indigo light. DMSO in the legend represents 1% DMSO ($n \geq 4$).

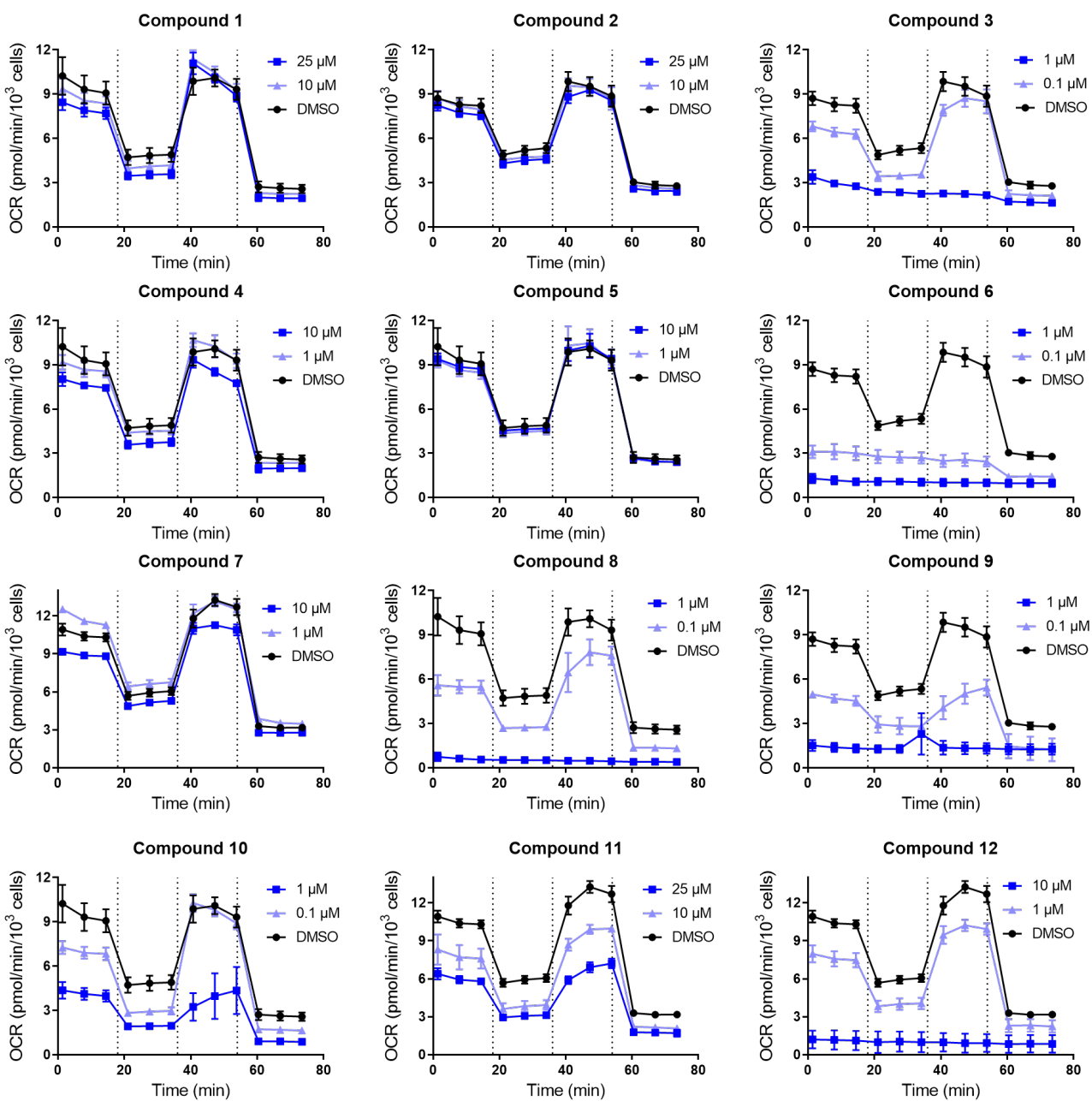


Figure S6. Extracellular flux analysis of compounds 1 – 12 following irradiation with indigo light (29.1 J/cm²). DMSO in the legend represents 1% DMSO (n ≥ 4).

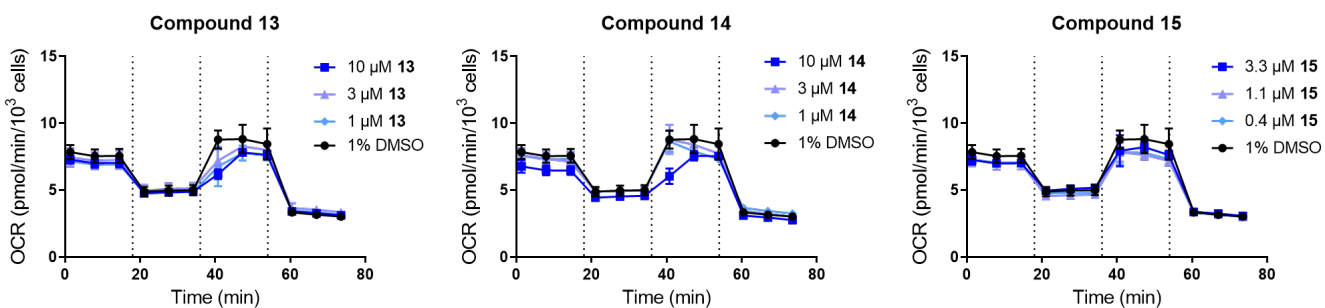


Figure S7. Extracellular flux analysis of compounds 13 – 15 (n ≥ 4).

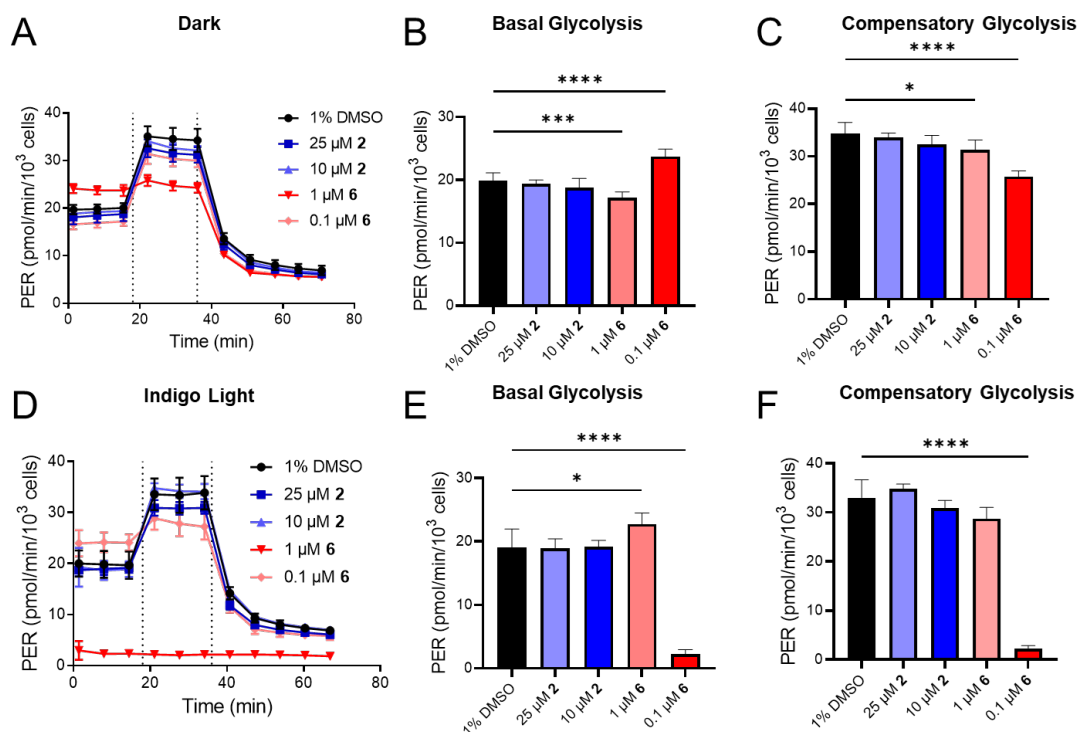


Figure S8. Glycolytic Rate Test following a 1 h incubation with **2** and **6**. **A)** Glycolytic rate following treatment with **2** and **6** in the dark. **B)** Basal glycolysis of 1% DMSO, **2**, and **6** treated cells in the dark. **C)** Compensatory glycolysis of 1% DMSO, **2**, and **6** treated cells in the dark. **D)** Glycolytic rate following treatment with **2** and **6** following irradiation with 450 nm light (29.1 J/ cm²). **E)** Basal glycolysis of 1% DMSO, **2**, and **6** treated cells following irradiation with 450 nm light (29.1 J/ cm²). **F)** Compensatory glycolysis of 1% DMSO, **2**, and **6** treated cells following irradiation with 450 nm light (29.1 J/ cm²) (n ≥ 4); *P < 0.05, **P < 0.01, ***P < 0.001, or ****P < 0.0001.

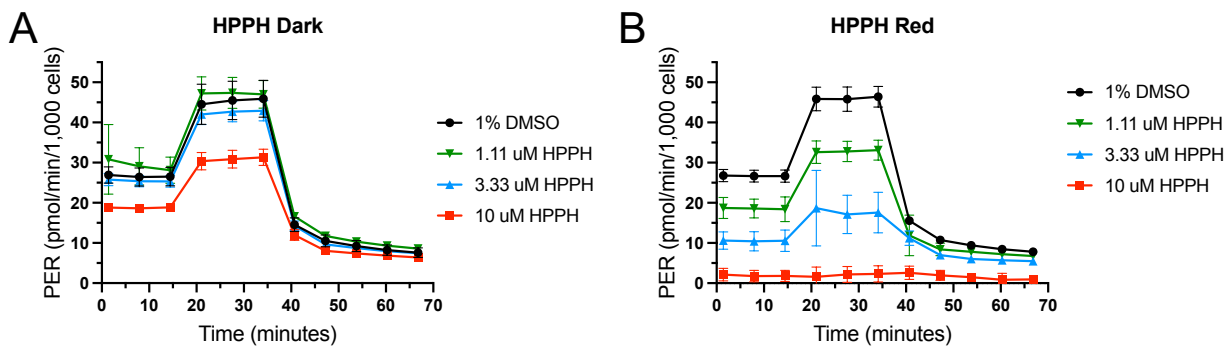


Figure S9. A) Glycolytic rate test for HPPH in the dark and B) irradiation with red light (660 nm, 57.8 J/cm²).

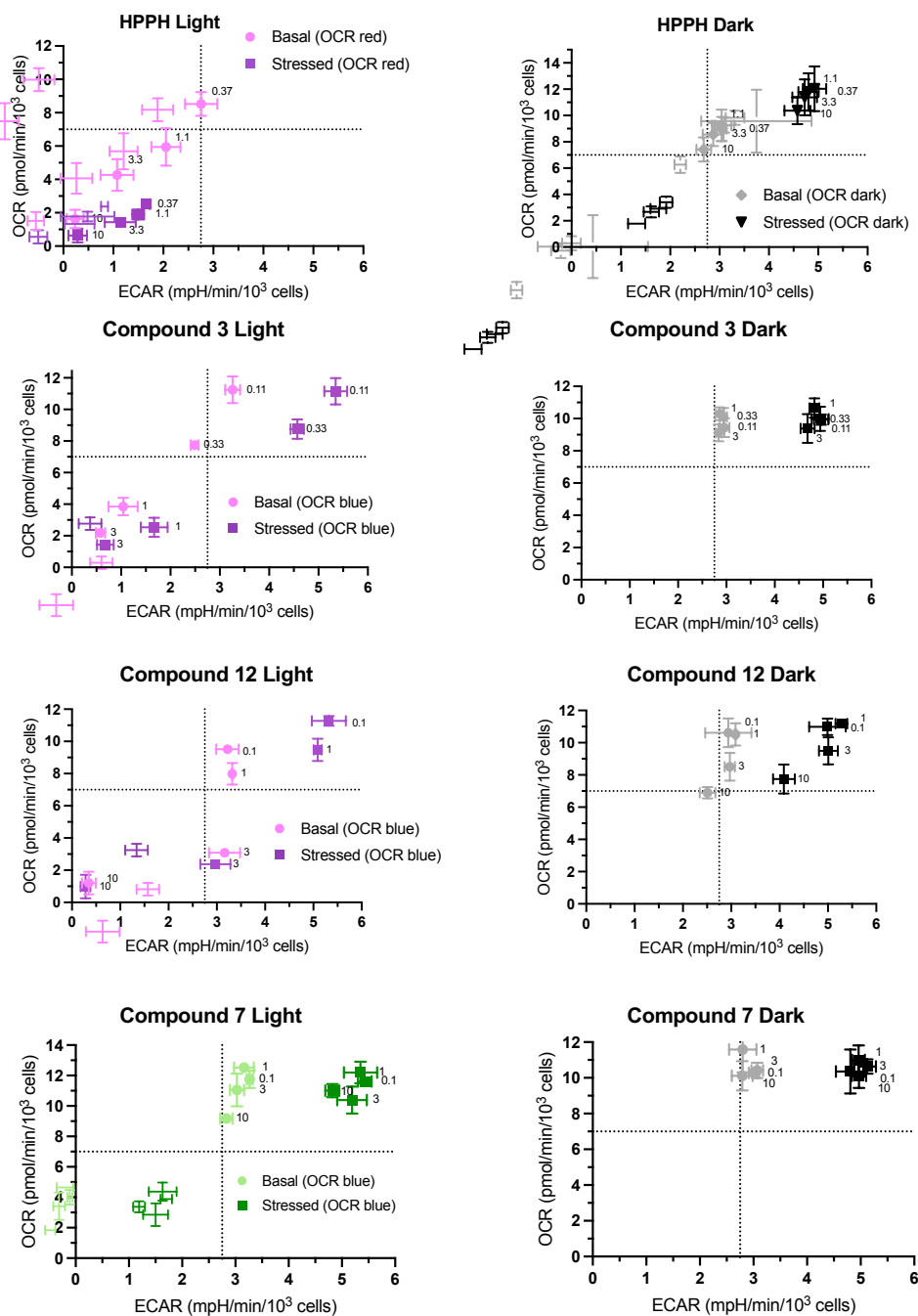


Figure S10. Concentration dependent bioenergetic impacts of phototherapeutics in A549 cells. The lighter colors reflect the basal phenotype (prior to the addition of oligomycin and FCCP), while darker colors represent the stressed phenotype (after oligomycin and FCCP but before addition of rotenone/antimycin A). Concentrations (in μM) indicated next to data points; $n > 3$ for Seahorse data. HPPH was activated with red light (660 nm , 57.8 J/cm^2) and all other compounds were activated with blue light (450 nm , 29.1 J/cm^2), or kept in the dark, as indicated. Compounds that can generate $^1\text{O}_2$ (purple) show a progressive shift to the quiescent phenotype, while compounds that photoeject (green) do not exhibit metabolic reprogramming.

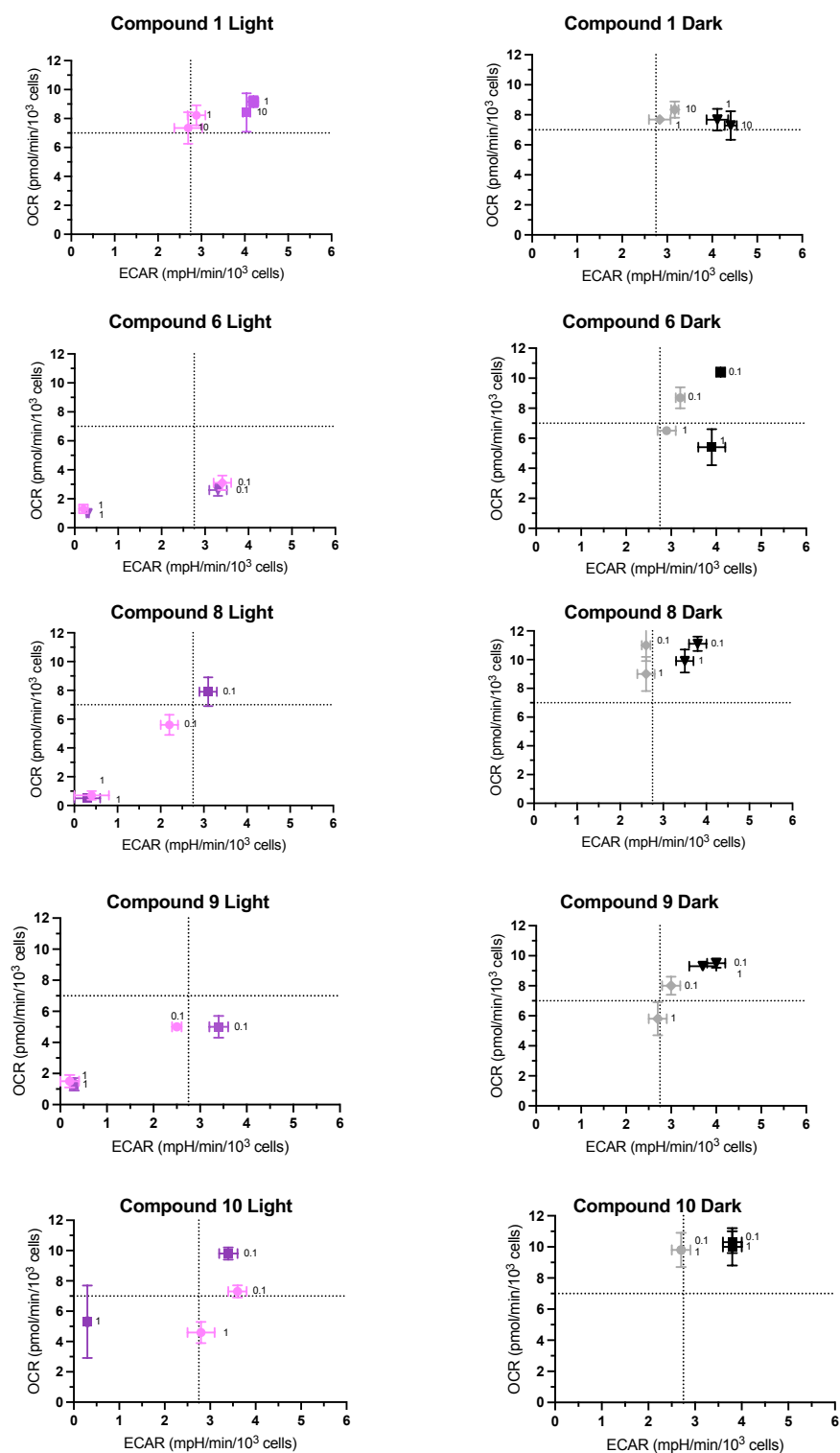


Figure S11. Concentration dependent bioenergetic impacts of compounds that can generate $^1\text{O}_2$ (purple) in A549 cells. The lighter colors reflect the basal phenotype (prior to the addition of oligomycin and FCCP), while darker colors represent the stressed phenotype (after oligomycin and FCCP but before addition of rotenone/antimycin A). Concentrations (in μM) indicated next to data points; $n > 3$ for Seahorse data. Compounds were activated with blue light (450 nm, 29.1 J/cm^2), or kept in the dark, as indicated.) A progressive shift to the quiescent phenotype is observed with these compounds.

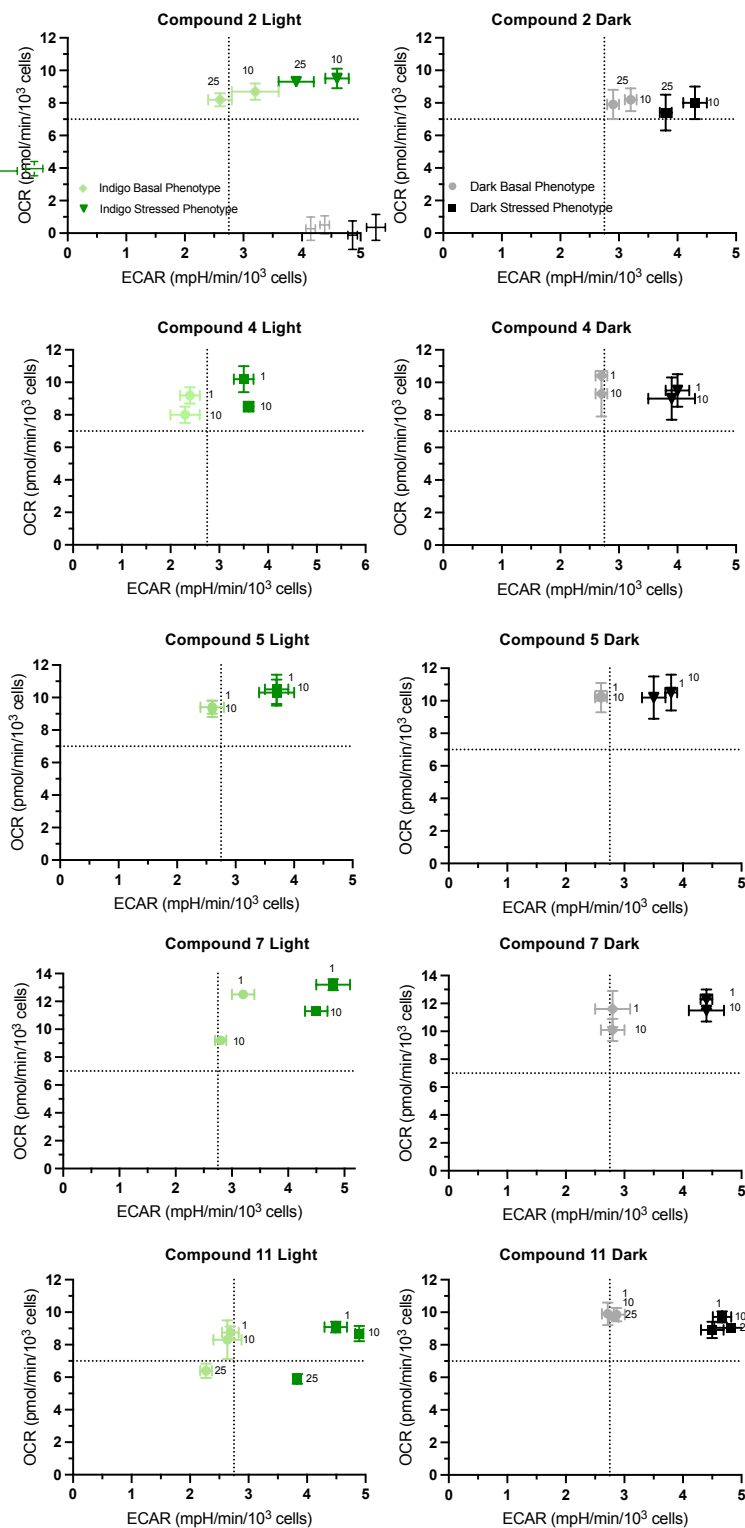


Figure S12. Concentration dependent bioenergetic impacts of compounds that photoeject (green) in A549 cells. The lighter colors reflect the basal phenotype (prior to the addition of oligomycin and FCCP), while darker colors represent the stressed phenotype (after oligomycin and FCCP but before addition of rotenone/antimycin A). Concentrations (in μM) indicated next to data points; $n > 3$ for Seahorse data. Compounds were activated with blue light (450 nm, 29.1 J/cm^2), or kept in the dark, as indicated.) Photoactivation has a minimal effect on the cellular metabolic profile.

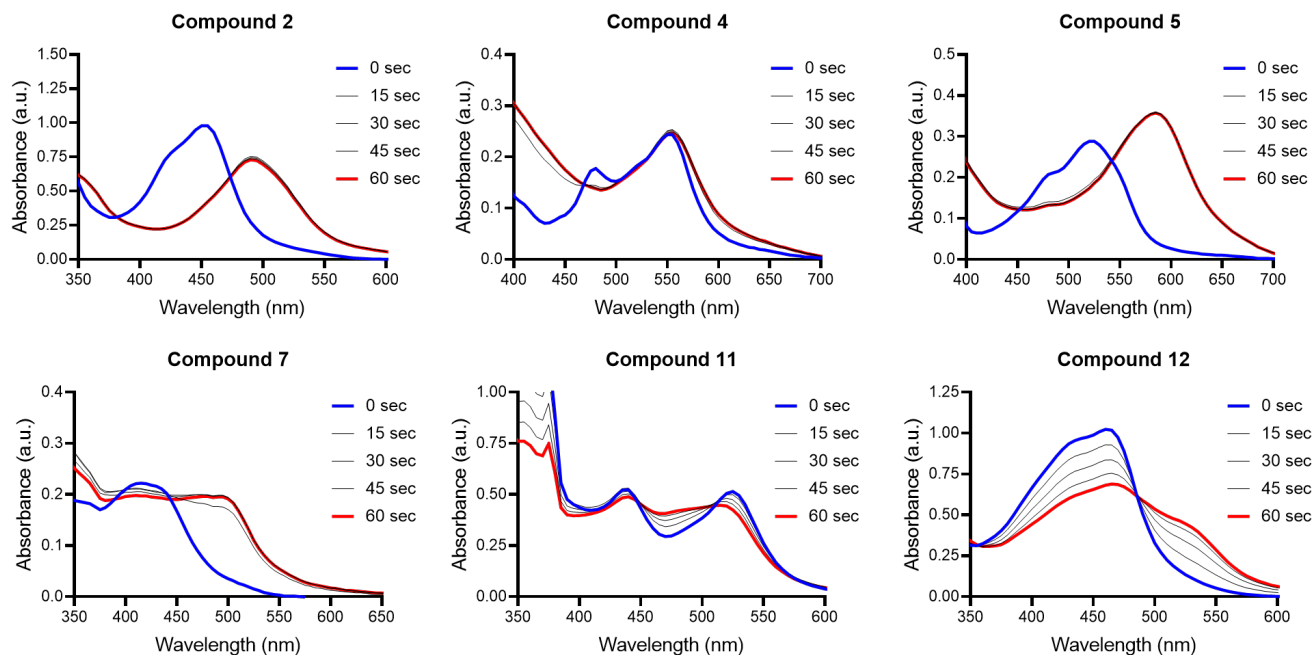


Figure S13. Photoejection UV/Vis of compounds **2**, **4**, **5**, **7**, **11**, and **12** in diH₂O at 50 μM over 60 seconds of irradiation with indigo light (450 nm) (n = 3).

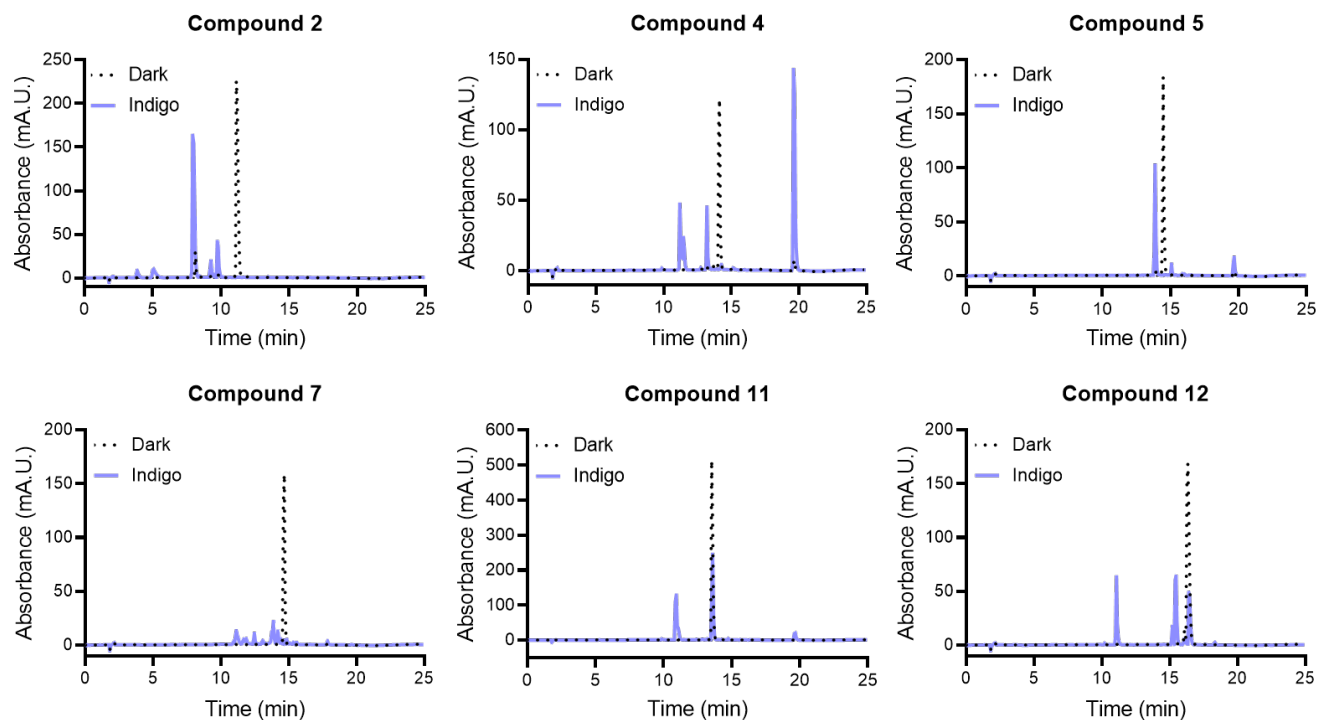


Figure S14. Photoejection of PACT compounds **2**, **4**, **5**, **7**, **11**, and **12**, kept in the dark or irradiated with Indigo light, monitored by HPLC. The chromatograms are representative of 100 μM solutions of each compound in water; irradiation was performed with 450 nm light (29.1 J/cm²).

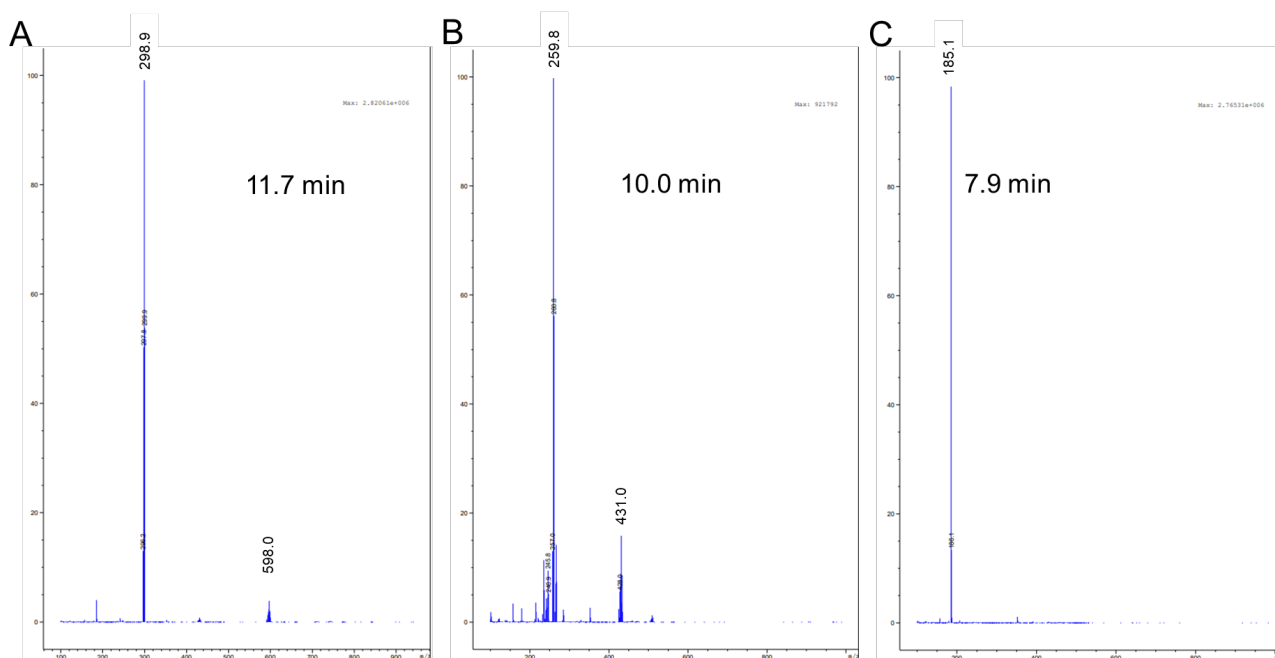


Figure S15. Mass spectra of the parent complex **2** and its photoejection products. **A)** Mass spectrum of **2**. **B)** Mass spectra of [Ru(bpy)₂(OH₂)₂]²⁺. **C)** Mass spectra of dmbpy. The retention times associated with each mass spectrum are indicated in the figure.

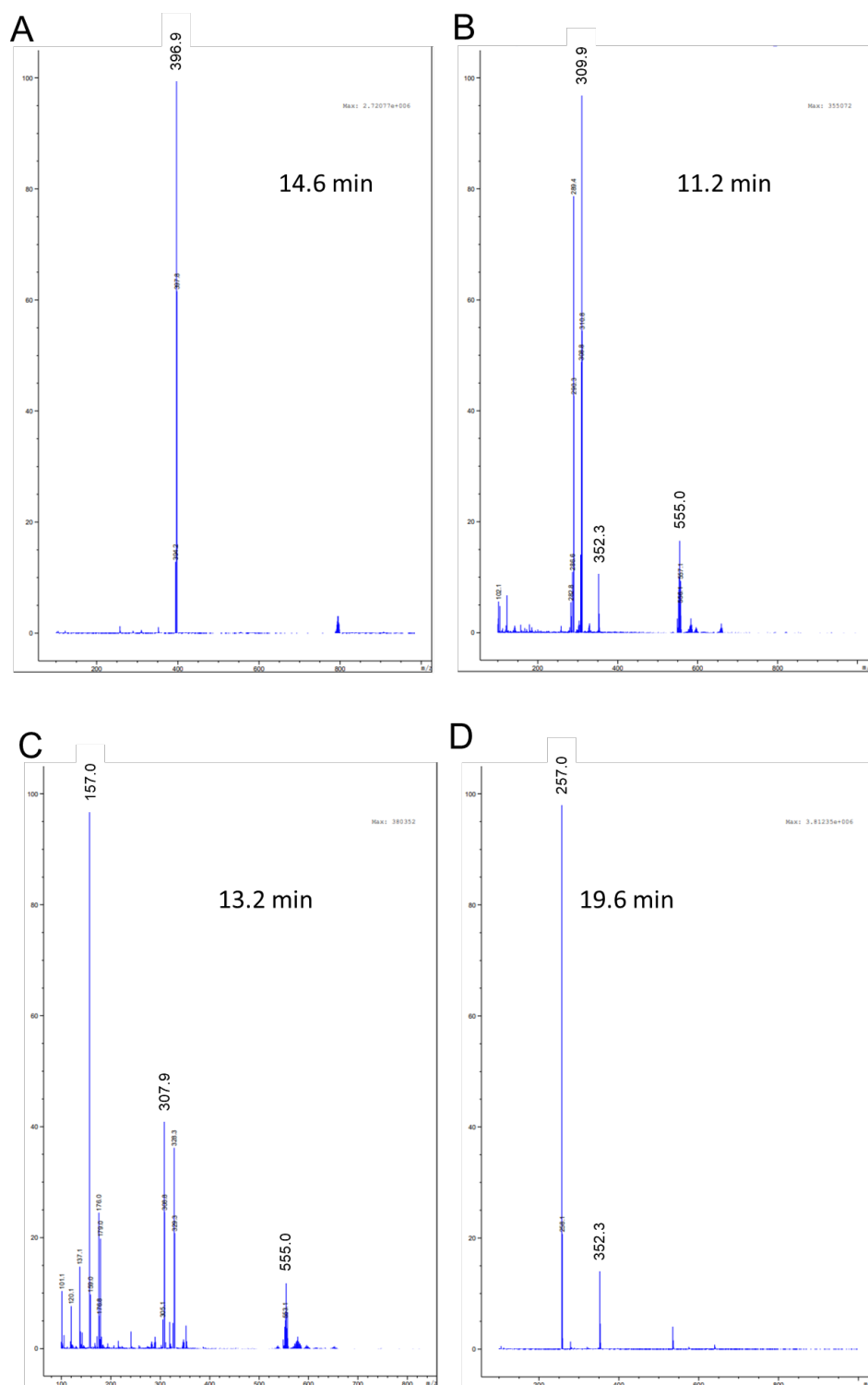


Figure S16. Mass spectra of the parent complex **4** and its photoejection products. **A)** Mass spectrum of **4**. **B)** Mass spectra of $[\text{Ru}(\text{biq})_2(\text{OH}_2)_2]^{2+}$. **C)** Mass spectrum of $\text{Ru}(\text{biq})_2(\text{MeCN})_2]^{2+}$. **D)** Mass spectrum of photoejected biq. The retention times associated with each mass spectrum are indicated in the figure. For B and C, other speciation products were present at low abundances. The m/z of 553.1 likely corresponds to $[\text{Ru}(\text{biq})(\text{MeCN})_4]\text{Cl}^+$.

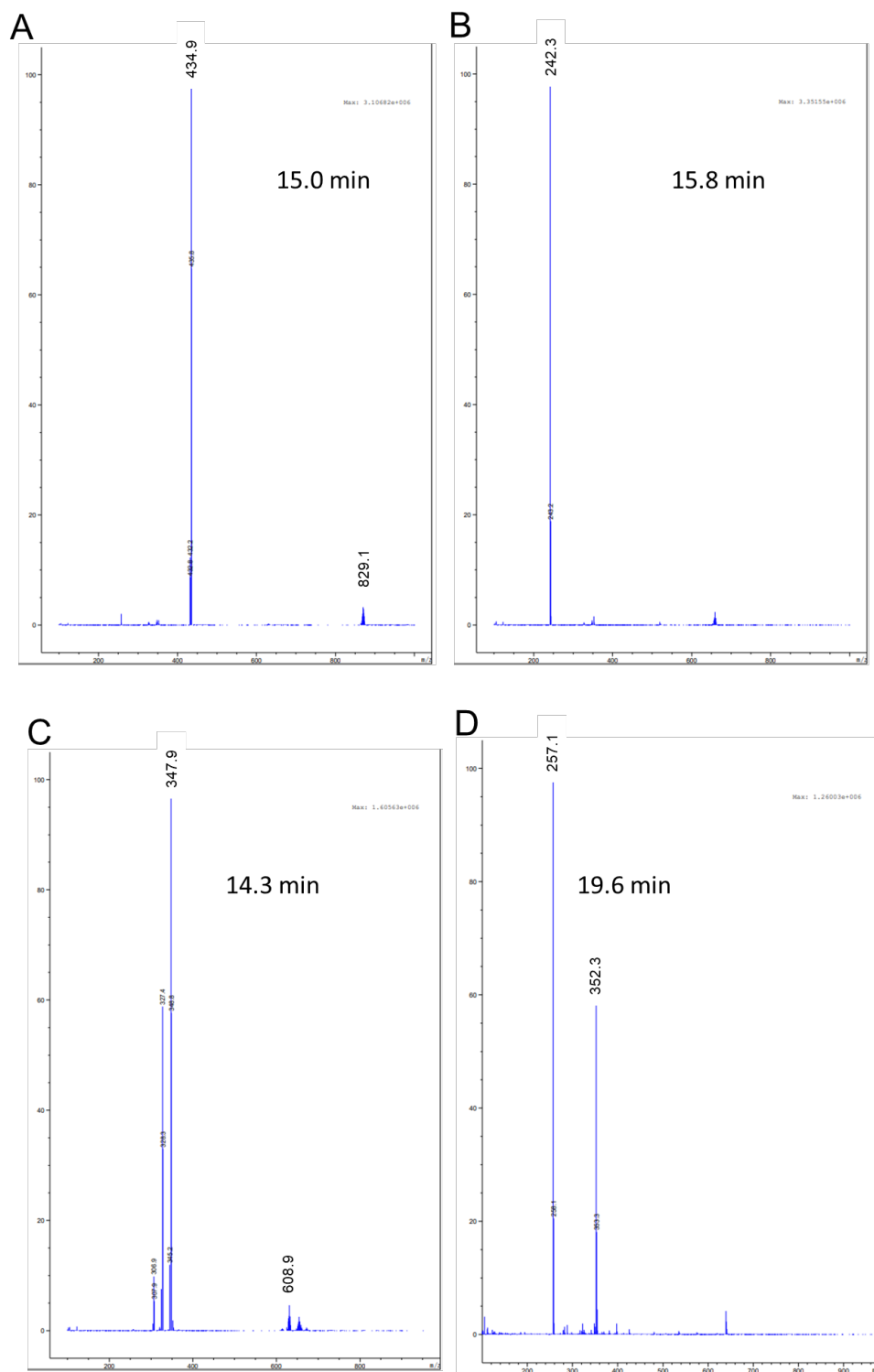


Figure S17. Mass spectra of the parent complex **5** and its photoejection products. **A)** Mass spectrum of **5**. **B)** Mass spectra of $[\text{Ru}(\text{biq})_2(\text{OH})_2]\text{Cl}^+$. **C)** Mass spectrum of $\text{Ru}(\text{biq})_2(\text{MeCN})_2\text{Cl}^+$. **D)** Mass spectrum of photoejected biq. The retention times associated with each mass spectrum are indicated in the figure. For B and C, other speciation products were present at low abundances.

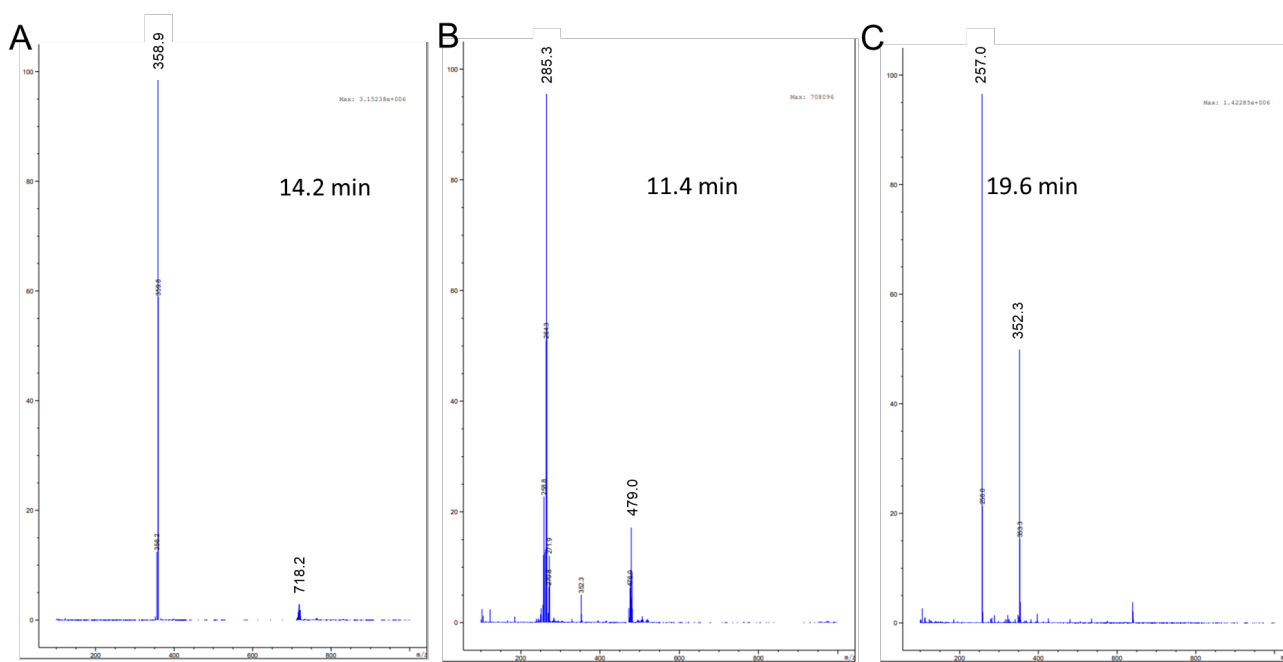


Figure S18. Mass spectra of the parent complex **11** and its photoejection products. **A)** Mass spectrum of **11**. **B)** Mass spectra of $[\text{Ru}(\text{phen})_2(\text{OH}_2)_2]^{2+}$ and $[\text{Ru}(\text{phen})_2(\text{MeCN})_2]^{2+}$. **C)** Mass spectra of dmbpy. The retention times associated with each mass spectrum are indicated in the figure.

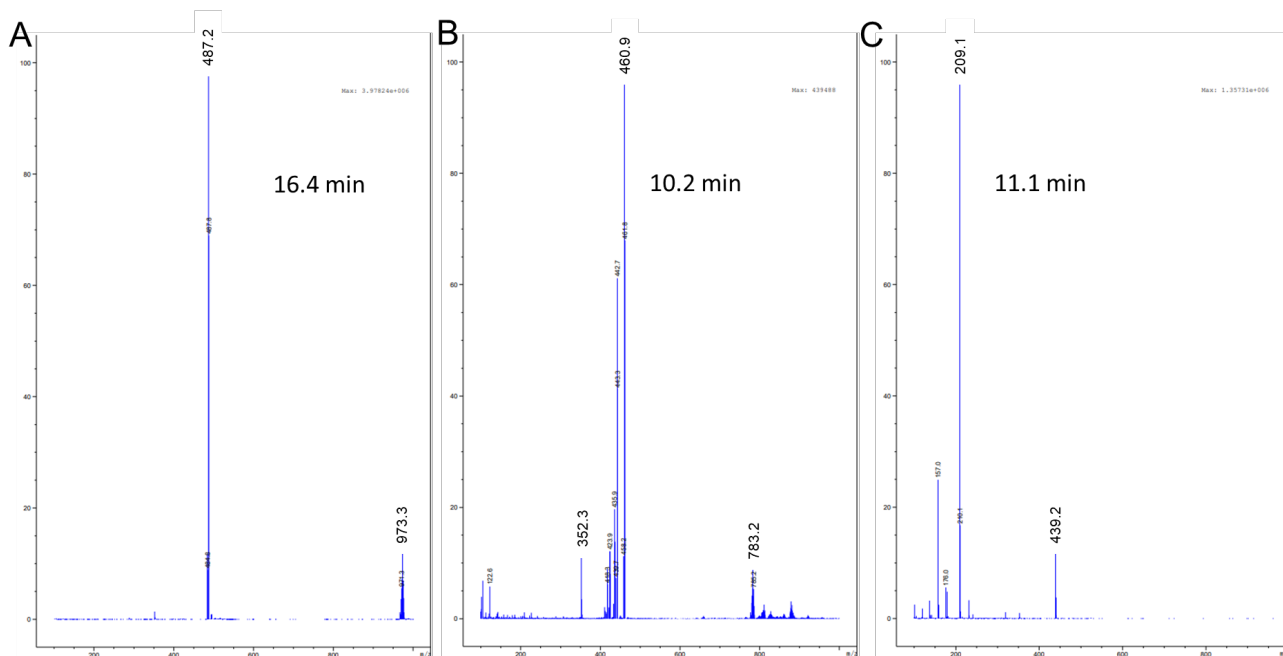


Figure S19. Mass spectra of the parent complex **12** and photoejection products. **A)** Mass spectrum of **12** as the PF_6 salt. **B)** Mass spectra of photoejected Ru(II) byproducts. **C)** Mass spectra of the protonated dmphen as indicated by the m/z of 209.1. The retention times associated with each mass spectrum are indicated in the figure.

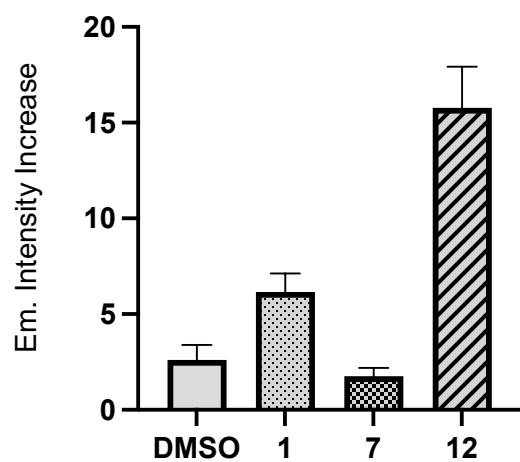


Figure S20. Light induced production of $^1\text{O}_2$ as detected by singlet oxygen sensor green (SOSG). The Y axis values are the ratio of the emission enhancement for the treated sample, exposed to 445 nm light for 2 min., vs. the sample before irradiation.

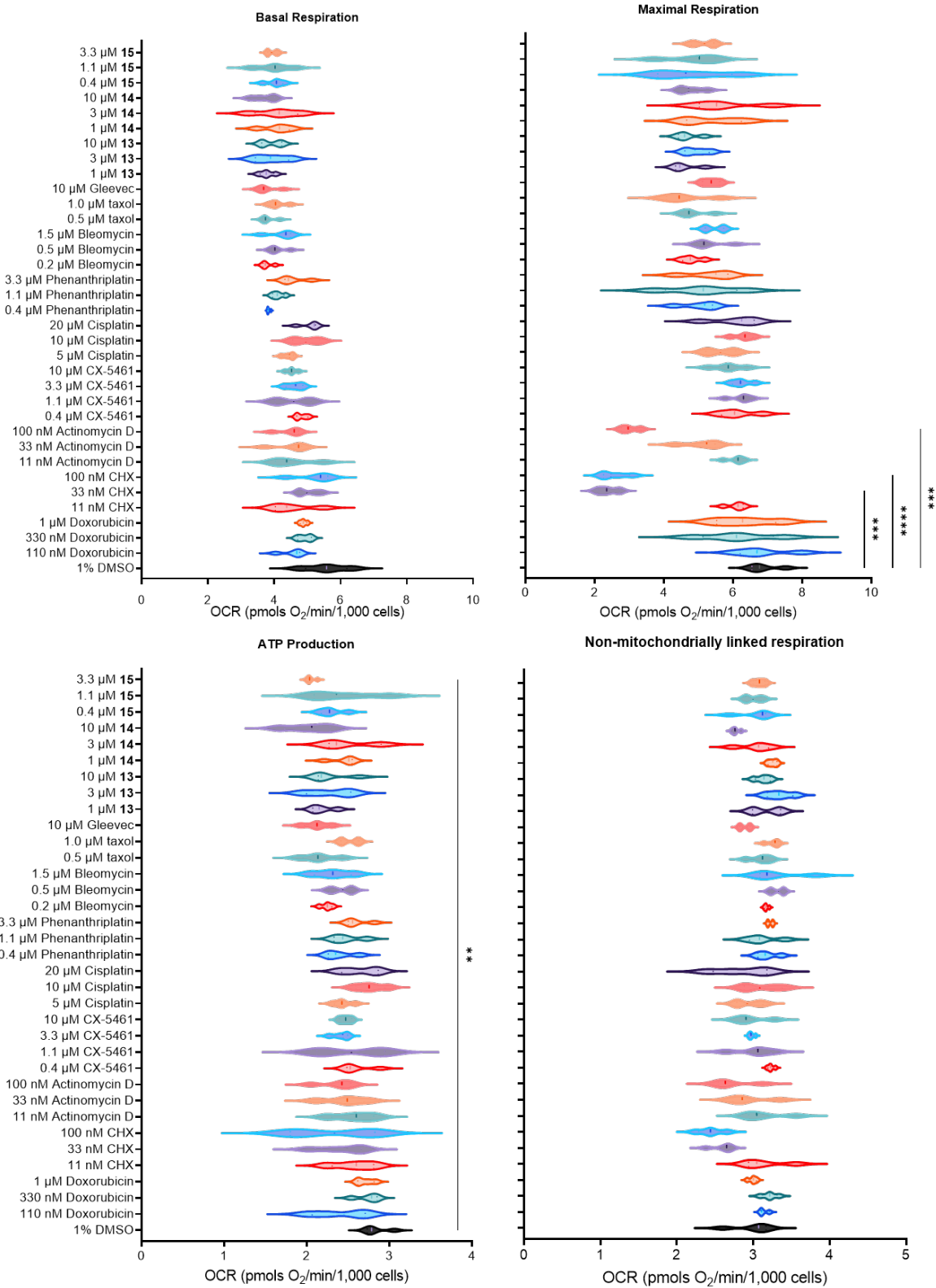


Figure S21. Key parameters of the MitoStress Test after a 1 h incubation with dark active compounds ($n \geq 4$); * $P < 0.05$, ** $P < 0.01$, *** $P < 0.001$, or **** $P < 0.0001$.

| Compound | 1 | 2 | 3 | 4 | 5 | 6 | 7 | 8 | 9 | 10 | 11 | 12 | 13 | 14 | 15 |
|--------------------------|------|------|------|------|------|------|------|------|------|------|------|------|------|------|------|
| Ret. Time (min) | 8.4 | 8.7 | 13.4 | 10.0 | 11.5 | 22.8 | 13.1 | 21.8 | 21.9 | 19.5 | 9.6 | 21.9 | 9.4 | 23.0 | 23.4 |
| Relative K _{ow} | 1.11 | 1.14 | 1.64 | 1.28 | 1.44 | 2.69 | 1.61 | 2.56 | 2.59 | 2.31 | 1.24 | 2.56 | 1.21 | 2.69 | 2.73 |

Table S2. Photoconversion of PACTs investigated.

| Compound | Percent Converted |
|-----------|-------------------|
| 2 | 100% |
| 4 | 99% |
| 5 | 100% |
| 7 | 96% |
| 11 | 39% |
| 12 | 72% |

Photoconversion was measured after irradiation with indigo light (29.1 J/cm²).

References

1. Park, G. Y.; Wilson, J. J.; Song, Y.; Lippard, S. J., Phenanthriplatin, a monofunctional DNA-binding platinum anticancer drug candidate with unusual potency and cellular activity profile. *Proc. Natl. Acad. Sci* **2012**, *109* (30), 11987- 11992.
2. Howerton, B. S.; Heidary, D. K.; Glazer, E. C., Strained Ruthenium Complexes Are Potent Light-Activated Anticancer Agents. *J. Am. Chem. Soc.* **2012**, *134*, 8324- 8327.
3. Wachter, E.; Heidary, D. K.; Howerton, B. S.; Parkin, S.; Glazer, E. C., Light-activated ruthenium complexes photobind DNA and are cytotoxic in the photodynamic therapy window. *Chem. Commun.* **2012**, *48* (77), 9649-9651.
4. Dickerson, M.; Sun, Y.; Howerton, B.; Glazer, E. C., Modifying Charge and Hydrophilicity of Simple Ru(II) Polypyridyl Complexes Radically Alters Biological Activities: Old Complexes, Surprising New Tricks. *Inorg. Chem.* **2014**, *53* (19), 10370-10377.
5. Havrylyuk, D.; Heidary, D. K.; Sun, Y.; Parkin, S.; Glazer, E. C., Photochemical and Photobiological Properties of Pyridyl-pyrazol(in)e-Based Ruthenium(II) Complexes with Sub-micromolar Cytotoxicity for Phototherapy. *ACS Omega* **2020**, *5* (30), 18894-18906.
6. Pyle, A. M.; Rehmann, J. P.; Meshoyrer, R.; Kumar, C. V.; Turro, N. J.; Barton, J. K., Mixed-ligand complexes of ruthenium(II): factors governing binding to DNA. *J. Am. Chem. Soc.* **1989**, *111* (8), 3051-3058.
7. Ryan, R. T.; Havrylyuk, D.; Stevens, K. C.; Moore, L. H.; Kim, D. Y.; Blackburn, J. S.; Heidary, D. K.; Selegue, J. P.; Glazer, E. C., Avobenzene incorporation in a diverse range of Ru(ii) scaffolds produces potent potential antineoplastic agents. *Dalton Trans.* **2020**, *49* (35), 12161-12167.